Article

Current Biology

The Conserved VPS-50 Protein Functions in Dense-Core Vesicle Maturation and Acidification and Controls Animal Behavior

Highlights

- *vps-50* affects the behavioral state of *C. elegans*
- VPS-50 and its murine homolog mVPS50 associate with synaptic and dense-core vesicles
- VPS-50 affects the maturation of dense-core vesicles
- VPS-50 and mVPS50 function in the acidification of synaptic and dense-core vesicles

Authors

Nicolas Paquin, Yasunobu Murata, Allan Froehlich, ..., Corinne L. Pender, Martha Constantine-Paton, H. Robert Horvitz

Correspondence

horvitz@mit.edu

In Brief

Paquin et al. show that the evolutionarily conserved protein VPS-50 regulates the behavioral state of *C. elegans* and the maturation of dense-core vesicles. VPS-50 and its murine homolog mVPS50 both function in the acidification of synaptic and dense-core vesicles, likely through regulation of the V-ATPase complex.

Paquin et al., 2016, Current Biology *26*, 862–871
April 4, 2016
http://dx.doi.org/10.1016/j.cub.2016.01.049

CellPress

CellPress

Current Biology
Article

The Conserved VPS-50 Protein Functions in Dense-Core Vesicle Maturation and Acidification and Controls Animal Behavior

Nicolas Paquin,[1,2] Yasunobu Murata,[1,2,3] Allan Froehlich,[1,2,4] Daniel T. Omura,[1,2,4] Michael Ailion,[5] Corinne L. Pender,[1,2] Martha Constantine-Paton,[1,2,3] and H. Robert Horvitz[1,2,4,*]

[1]Department of Biology, Massachusetts Institute of Technology, 77 Massachusetts Avenue, Cambridge, MA 02139, USA
[2]McGovern Institute for Brain Research, Massachusetts Institute of Technology, 77 Massachusetts Avenue, Cambridge, MA 02139, USA
[3]Department of Brain and Cognitive Science, Massachusetts Institute of Technology, 77 Massachusetts Avenue, Cambridge, MA 02139, USA
[4]Howard Hughes Medical Institute, Massachusetts Institute of Technology, 77 Massachusetts Avenue, Cambridge, MA 02139, USA
[5]Department of Biochemistry, University of Washington, 1705 NE Pacific Street, Seattle, WA 98195, USA
*Correspondence: horvitz@mit.edu
http://dx.doi.org/10.1016/j.cub.2016.01.049

SUMMARY

The modification of behavior in response to experience is crucial for animals to adapt to environmental changes. Although factors such as neuropeptides and hormones are known to function in the switch between alternative behavioral states, the mechanisms by which these factors transduce, store, retrieve, and integrate environmental signals to regulate behavior are poorly understood. The rate of locomotion of the nematode *Caenorhabditis elegans* depends on both current and past food availability. Specifically, *C. elegans* slows its locomotion when it encounters food, and animals in a food-deprived state slow even more than animals in a well-fed state. The slowing responses of well-fed and food-deprived animals in the presence of food represent distinct behavioral states, as they are controlled by different sets of genes, neurotransmitters, and neurons. Here we describe an evolutionarily conserved *C. elegans* protein, VPS-50, that is required for animals to assume the well-fed behavioral state. Both VPS-50 and its murine homolog mVPS50 are expressed in neurons, are associated with synaptic and dense-core vesicles, and control vesicle acidification and hence synaptic function, likely through regulation of the assembly of the V-ATPase complex. We propose that dense-core vesicle acidification controlled by the evolutionarily conserved protein VPS-50/mVPS50 affects behavioral state by modulating neuropeptide levels and presynaptic neuronal function in both *C. elegans* and mammals.

INTRODUCTION

Like other animals, *Caenorhabditis elegans* modulates its behavior in response to both environmental signals and past experience [1, 2]. For example, both well-fed and food-deprived worms slow their locomotion after encountering food, and well-fed worms slow less than food-deprived worms (Figure 1A), presumably because food-deprived animals have a greater need to be in the proximity of food. The responses of well-fed and food-deprived worms upon encountering food require different sets of genes, neurotransmitters, and neurons, indicating that these responses reflect two distinct behavioral states [1, 2]. The mechanisms by which animals integrate information about their current environment and their past experience to modulate behavior are poorly understood.

Mutations that impair the maturation of dense-core vesicles and neuropeptide signaling alter the locomotion behavior of *C. elegans* [3]. Whereas synaptic vesicles transport and release neurotransmitters, such as acetylcholine, GABA, and glutamate, dense-core vesicles transport and release neuromodulators, such as biogenic amines and neuropeptides. In mammals, specific neuropeptides have been associated with the assumption of one of two alternative behavioral states, including hunger-satiety and sleep-wakefulness [4, 5].

From genetic screens, we isolated mutants of *C. elegans* that behave similarly whether they have been well fed or food deprived. We have characterized one gene defined by these mutations, *vps-50*, and show that although *vps-50* mutants behave as though they have been food deprived, they are not malnourished but rather failing to switch behavioral states: they behave as though food deprived even when well fed. We describe below the characterization of both *C. elegans* VPS-50 and its murine homolog, mVPS50, and show that both function in dense-core vesicle maturation and acidification.

RESULTS

vps-50 Regulates *C. elegans* Behavior

To understand the mechanisms that control the behavioral states of *C. elegans* in response to food availability and past feeding experience, we have characterized three allelic mutations, *ox476*, *n3925*, and *n4022*, that cause well-fed animals to behave as though they had been food deprived (Figure 1A). *ox476*, *n3925*, and *n4022* are alleles of an evolutionarily conserved gene, *C44B9.1*, which we have named *vps-50* (see below) (Figure S1). *vps-50* mutants have normal rates of

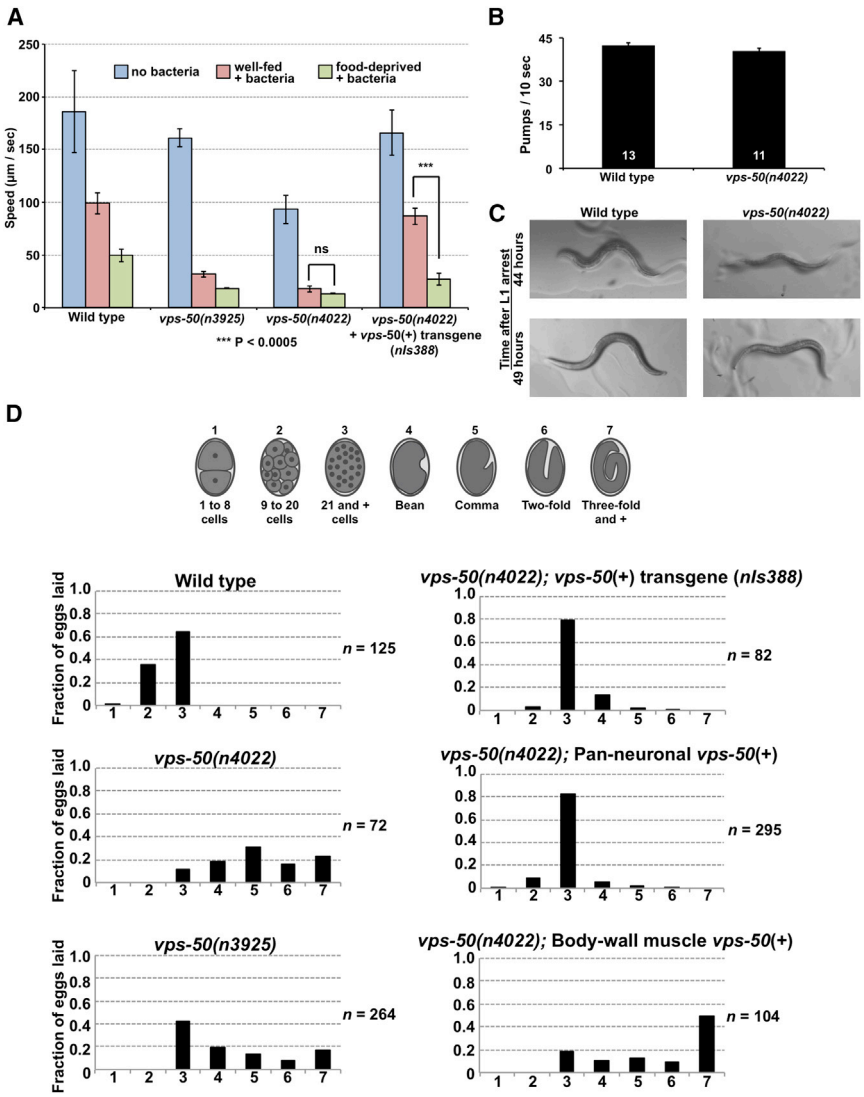

Figure 1. VPS-50 Regulates the Behavioral State of *C. elegans*

(A) The locomotory behavior of *C. elegans* is modulated by the presence of food and past feeding experience. Well-fed wild-type animals move more slowly on a bacterial lawn (red bars) than in the absence of bacteria (blue bars), and food-deprived animals (green bars) slow even more than well-fed animals [1]. *vps-50* mutants (*n3925* and *n4022*) moved as though they were food deprived even when well fed, and this behavioral defect was rescued by a transgene expressing a GFP-tagged wild-type copy of *vps-50* from its endogenous promoter. n = 6 plates for the wild-type; n = 3 plates for all other genotypes. Means ± SDs. ns, not significant.

(B) *vps-50* mutants show normal pumping rates, indicating that they do not have a feeding defect.

(C) *vps-50* mutants develop at a rate similar to that of wild-type animals. We followed synchronized animals after recovery from L1 arrest. All wild-type and *vps-50* mutant worms observed had a developed vulva after 44 hr; 12/12 wild-type animals were gravid after 49 hr, whereas 11/12 *vps-50* mutants were gravid after 49 hr.

(D) Analyses of the in utero retention time of eggs, assayed by the distribution of the developmental stages of newly laid eggs. *vps-50* mutants retained eggs in utero for an abnormally long period of time, as seen by a shift to later stages of their newly laid eggs. The egg-laying defect of *vps-50* mutants was rescued by transgenes expressing *vps-50* under its endogenous promoter or a pan-neuronal promoter, but not under a body-wall muscle promoter.

See also Figure S1.

pharyngeal pumping and do not display the slow growth and abnormal pigmentation of starved wild-type animals (Figures 1B and 1C), indicating that *vps-50* mutants are not malnourished but rather are in the behavioral state normally induced by acute food deprivation. *vps-50* mutants are abnormal not only in locomotion but also in egg laying, as they retain eggs for an abnormally long period of time and lay eggs at substantially later developmental stages than do wild-type worms (Figure 1D). Food-deprived wild-type worms are similarly abnormal in egg laying, further indicating that *vps-50* mutants are in a food-deprived state when not food deprived.

vps-50 Acts in Neurons to Control *C. elegans* Behavior

We examined the expression pattern of a transgene that expresses a VPS-50::GFP fusion under the control of the *vps-50* promoter and observed that *vps-50* is expressed broadly in the nervous system and possibly in all neurons (Figure 2; data not shown). These observations suggest that *vps-50* plays a specific role in neuronal function. To determine where *vps-50* functions, we used transgenes that express *vps-50* in a tissue-specific manner and attempted to rescue the mutant phenotype of *vps-50* mutants. Expression of *vps-50* using the *rab-3* pan-neuronal promoter significantly rescued both the locomotion and egg-laying defects of *vps-50(n4022)* mutants, whereas expression in body-wall muscles using the *myo-3* promoter failed to rescue the locomotion and egg-laying defects of *vps-50* mutants (Figures 1D and 2B). We conclude that *vps-50* functions in neurons.

To analyze further the cellular sites of function of VPS-50 in the nervous system, we expressed *vps-50* in subsets of neurons. VPS-50 expression in cholinergic neurons in *vps-50* mutants using the *unc-17* promoter rescued the locomotion defect of well-fed *vps-50* mutant worms in the presence of food, whereas *vps-50* expression in GABAergic neurons using the *unc-47* promoter did not improve the locomotion of well-fed *vps-50* mutants in the presence of food (Figure 2C). These observations suggest that *vps-50* functions in cholinergic neurons to control locomotion. Expression of *vps-50* using the *tax-2* promoter, which drives expression in the main sensory neurons that control olfaction, gustation, and thermotaxis, did not rescue the locomotion defect of *vps-50* mutant worms, suggesting that this behavioral defect of *vps-50* mutants is not a consequence of altered food sensing (Figure 2C).

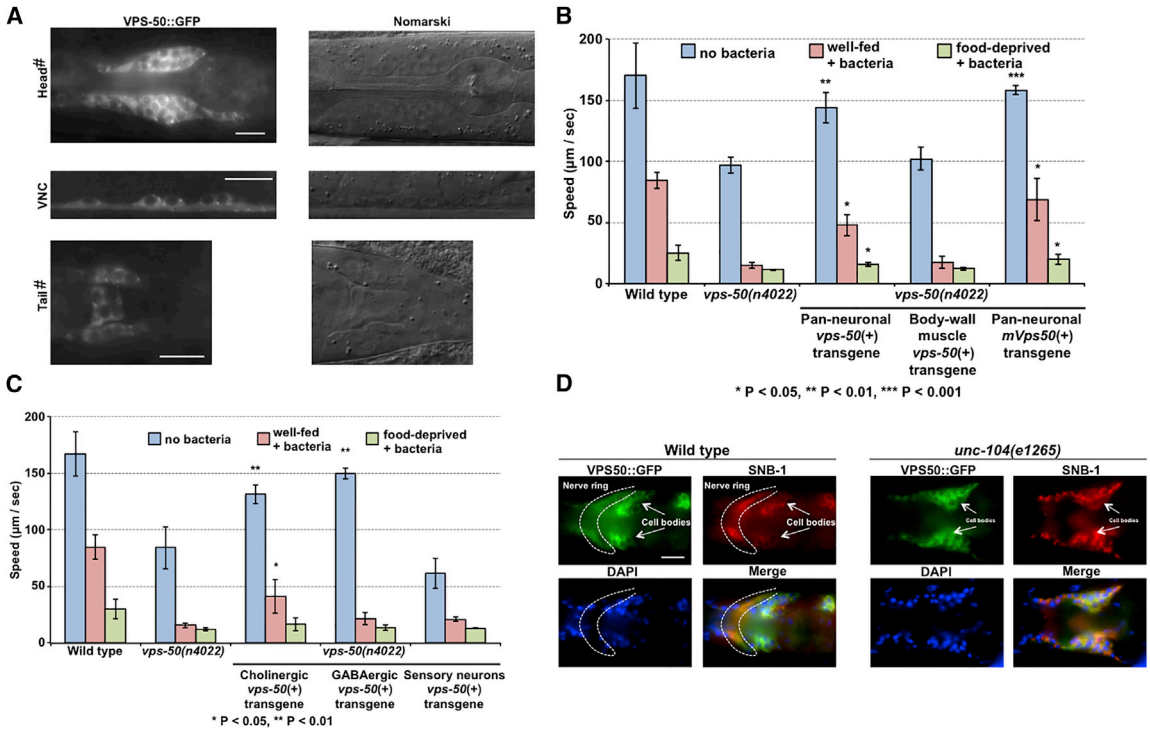

Figure 2. VPS-50 Functions in Neurons

(A) Fluorescence and Nomarski micrographs of regions of *C. elegans* transgenic animals expressing VPS-50::GFP (*nIs388*) using the *vps-50* promoter. *vps-50* was expressed in most, if not all, neurons. Occasional expression was observed in some pharyngeal muscles. VNC, ventral nerve cord. #To enhance visualization, we used *unc-104(e1265)* mutant animals to increase the fluorescence level in cell bodies. Scale bars, 10 μm.

(B) *vps-50* functions in neurons to regulate locomotion. *vps-50* was expressed pan-neuronally (*Prab-3*) and in body-wall muscles (*Pmyo-3*) to identify its site of action. Pan-neuronal expression of *vps-50*, or of its murine homolog *mVps50*, rescued the locomotion defect of *vps-50(n4022)* animals. n = 3 plates for all genotypes.

(C) *vps-50* functions in cholinergic neurons to regulate locomotion on food. *vps-50* was expressed in cholinergic neurons (*Punc-17*), in GABAergic neurons (*Punc-47*), and in a subset of sensory neurons (*Ptax-2*) to identify its site of action. n = 5 plates for the wild-type and *vps-50(n4022)*; n = 3 plates for all other genotypes.

(B and C) Significance is defined by comparison to the equivalent state for *vps-50(n4022)* mutants. Means ± SDs.

(D) The localization of VPS-50::GFP to synapse-rich areas of the nerve ring depends on UNC-104/KIF1A, a molecular motor that transports synaptic vesicles and their associated proteins to synapses. Immunohistochemistry against GFP and synaptobrevin (SNB-1) and DAPI staining are shown. The dotted lines indicate the synapse-rich nerve ring, and clusters of neuronal cell bodies are marked. Scale bar, 10 μm.

VPS-50 is highly conserved from worms to mammals (Figure S1B), and pan-neuronal expression in *vps-50* mutant worms of its murine homolog mCCDC132, which we refer to as mVPS50, rescued the locomotion defect of *vps-50* mutants (Figure 2B). Thus, *C. elegans* VPS-50 and murine mVPS50 not only are similar in sequence but also are functionally similar and likely act in similar molecular processes.

VPS-50 and Its Murine Homolog Associate with Synaptic Vesicles

Using an anti-GFP antibody to visualize a VPS-50::GFP fusion protein in *C. elegans* whole mounts, we observed VPS-50::GFP in neuronal cell bodies and also at synapse-rich regions such as the nerve ring (Figure 2D). In *C. elegans*, both synaptic and dense-core vesicles as well as their associated proteins are transported to synapses by the kinesin-like protein UNC-104/KIF1A [6, 7]. Like the transport of the vesicular SNARE protein synaptobrevin (SNB-1), the transport of VPS-50 to the nerve ring required UNC-104/KIF1A, suggesting that VPS-50 associates with synaptic or dense-core vesicles (Figure 2D).

The mammalian *Vps50* gene (also known as *CCDC132* or *Syndetin*) has been reported to be highly expressed in many regions of both the mouse and human brains [8]. Using an antibody against VPS50, we determined that the mVPS50 protein is widely expressed in the mouse brain throughout development (Figures 3A–3C) and in most and possibly all excitatory and inhibitory neurons (Figure 3D). We examined the distribution of mVPS50 in mouse cultured primary cortical and hippocampal neurons. mVPS50 did not colocalize with the *cis*-Golgi apparatus marker GM130 (Figure 4A) but did substantially colocalize with the *trans*-Golgi markers Golgin-97 and TGN38 (Figures 4B and S3A). These observations suggest that mVPS50 is at least partially localized to the *trans*-Golgi. The *trans*-Golgi apparatus has been proposed to be the final sorting compartment for both synaptic and dense-core vesicles [10]. Based on this information and our observation that *C. elegans* VPS-50 associates with synaptic or dense-core vesicles, we analyzed the colocalization

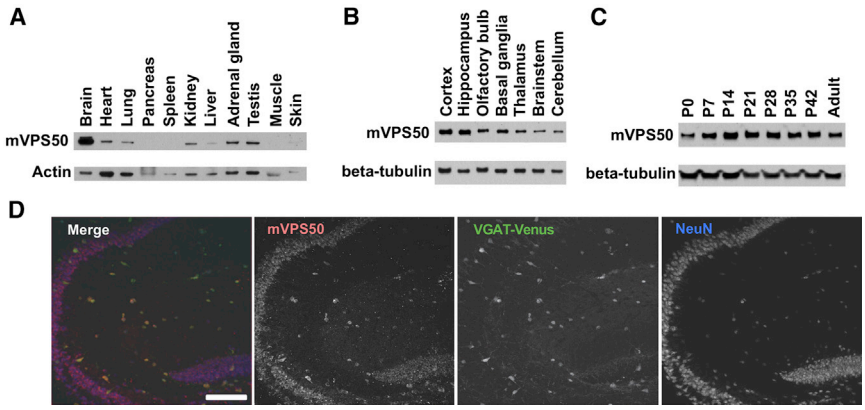

Figure 3. mVPS50 Is Widely Expressed in Mammalian Brain Neurons

Anti-VPS50 antibodies specifically recognize mVPS50 (see Figure S2 for validation of the anti-mVPS50 antibody).

(A) mVPS50 is enriched in brain tissue. Protein extracts from dissected adult mouse tissues were analyzed for mVPS50 expression by immunoblotting.

(B) mVPS50 is expressed in most brain regions, with strong expression in cortex and hippocampus.

(C) mVPS50 is expressed in mouse cortex throughout postnatal (P) development. Protein extracts from dissected mouse cortex were analyzed for mVPS50 expression at different developmental stages.

(D) mVPS50 is expressed broadly in mouse hippocampal neurons. Transgenic mice that express VGAT-Venus in inhibitory neurons were used for immunohistochemical studies of sagittal hippocampal slices [9]. The dentate gyrus and CA3 are shown. The mVPS50 immunostaining overlaps with the neuron-specific marker NeuN, including both Venus-positive inhibitory neurons and Venus-negative excitatory neurons. Scale bar, 100 μm.

See also Figure S2.

of mVPS50 with dense-core vesicles in mouse cultured primary neurons. mVPS50 colocalized with dense-core vesicles that contained Chromogranin C or neuropeptide Y (Figures 4C and 4D). The mVPS50 signal did not extend as far in the neuronal processes as did the neuropeptide signals, so it is possible that the colocalization observed between mVPS50 and neuropeptides is limited to the *trans*-Golgi apparatus and to early vesicles budding from it.

We fractionated extracts of adult mouse cortex and showed that mVPS50 was enriched in a fraction that contained synaptic and dense-core vesicles (LP2), suggesting that, like *C. elegans* VPS-50, the murine protein is associated with synaptic or dense-core vesicles (Figure 4E). The LP2 fraction, which is the pellet obtained after centrifugation of fraction LS1, also contained neuropeptides, as indicated by the detection of Chromogranin C. We further fractionated the synaptic vesicle and cytosol LS1 fraction using a sucrose density gradient. The distribution of mVPS50 is like that of the clathrin heavy chain, which assembles onto vesicle membranes, and not like that of the membrane-bound synaptophysin or that of the neuropeptide Chromogranin C (Figure 4F). We concluded that mVPS50 likely associates with synaptic vesicles as a soluble protein and is not in the lumen of vesicles or integrated into synaptic and dense-core vesicle membranes. We have not observed VPS-50 or mVPS50 at synapses in *C. elegans* or in mouse cultured primary neurons, respectively, indicating that these proteins likely associate with immature synaptic and dense-core vesicles budding from the *trans*-Golgi but do not traffic all the way to mature synapses (data not shown).

vps-50 Mutant Animals Have a Defect in Dense-Core Vesicle Maturation

The behavioral defects of *vps-50* mutant worms are strikingly similar to those of mutants in *unc-31* (the worm homolog of mammalian CADPS2/CAPS), *rab-2* (the homolog of RAB2, which is also known as *unc-67* and *unc-108* in *C. elegans*), and *rund-1* (the ortholog of RUNDC1), genes involved in the release and maturation of dense-core vesicles, but not like those of animals mutant for *egl-3*, which encodes a proprotein convertase that cleaves neuropeptides (Figures 5A and S4) [3, 11–14]. *unc-31* affects the release of dense-core, but not of synaptic vesicles [12], suggesting that VPS-50 functionally affects dense-core vesicles. Dense-core vesicles release biogenic amines and neuropeptides. *cat-2* and *tph-1* mutants, which are deficient in the synthesis of dopamine and serotonin, respectively, and *cat-2 tph-1 tdc-1* triple mutant animals, which are defective for the synthesis of all known biogenic amines in *C. elegans* [15–17], did not display the *vps-50* mutant phenotype (Figure 5B), suggesting that VPS-50 functions in neuropeptide signaling.

To determine whether *vps-50* affects neuropeptides, we used a FLP-3::Venus neuropeptide fusion protein to analyze neuropeptide levels, localization, release, and processing [13]. *unc-31* (CADPS2/CAPS) mutants, which are impaired in the release of dense-core vesicles [12], and *egl-3* (PC2) mutants, which are impaired in the processing of neuropeptides [18], accumulated elevated levels of FLP-3::Venus at synapses in the dorsal nerve cord. By contrast, *rab-2* mutants, which are defective in dense-core vesicle maturation, have been reported to have decreased levels of neuropeptides at synapses [13]. *vps-50* mutants, like *rab-2* mutants, had decreased levels of FLP-3::Venus at synapses, revealing that *vps-50* function is necessary for normal levels of synaptic neuropeptides (Figure 5C). The FLP-3::Venus fusion did not significantly accumulate in cell bodies of *vps-50* mutants, indicating that their low levels of neuropeptides at synapses were not the result of a transport defect (Figure 5D).

Synaptic levels of neuropeptides could be low in *vps-50* mutants either because of defects in producing neuropeptides or because these mutants degrade or release neuropeptides faster than wild-type animals. To assess the rate of neuropeptide release, we quantified FLP-3::Venus levels in coelomocytes, scavenger cells that take up secreted proteins from the worm's body cavity [19]. Neuropeptide levels in coelomocytes correlate with the neuropeptide levels released from neurons [12, 20]. Coelomocytes in *vps-50* mutants exhibited abnormally low levels of FLP-3::Venus (Figure 5E), indicating that *vps-50* mutants are not secreting neuropeptides faster than do wild-type animals. Taken together, these results suggest that

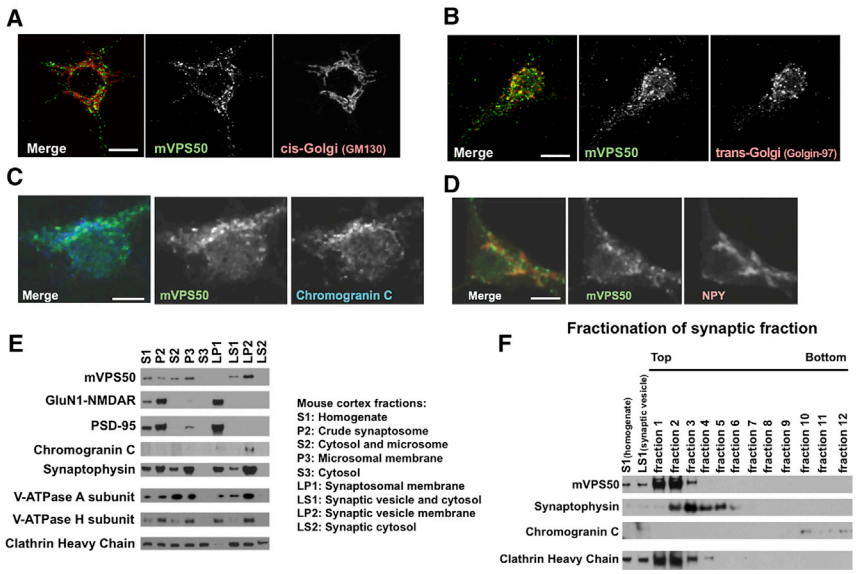

Figure 4. mVPS50 Associates with Synaptic and Dense-Core Vesicles

(A) mVPS50 does not colocalize with the *cis*-Golgi apparatus (GM130) in mouse primary cultured cortical neurons.

(B) mVPS50 partially colocalizes with the *trans*-Golgi apparatus (Golgin-97) in mouse primary cultured cortical neurons.

(C) mVPS50 partially colocalizes with Chromogranin C-containing dense-core vesicles (ChrC) in mouse primary cultured cortical neurons.

(D) mVPS50 partially colocalizes with neuropeptide Y-containing dense-core vesicles (NPY) in mouse primary cultured cortical neurons.

(A–D) Endogenous mVPS50, GM130, Golgin-97, ChrC, and NPY were detected by immunofluorescence. Scale bars, 10 μm (A and B) and 5 μm (C and D).

(E) mVPS50 significantly cofractionates with the synaptic vesicle protein synaptophysin and the neuropeptide Chromogranin C. Extracts from adult mouse cortex were fractionated, and fractions were probed by immunoblotting for mVPS50, the NMDA glutamate receptor subunit GluN1, the post-synaptic density protein PSD-95, the neuropeptide Chromogranin C, the synaptic vesicle membrane protein synaptophysin, the cytoplasmic V-ATPase A and H subunits (the mammalian homolog of *C. elegans* VHA-15), and the vesicle coat protein clathrin heavy chain.

(F) mVPS50 is a soluble protein. The synaptic vesicle and cytosol (LS1) fraction from adult mouse cortex was further fractionated using sucrose gradient centrifugation, and fractions were probed by immunoblotting.

See also Figure S3.

vps-50 mutants, like *rab-2* mutants, produce low levels of neuropeptides. The effect of *vps-50* on neuropeptide levels at synapses is not limited to FLP-3, as an NLP-21::Venus reporter also showed low levels at synapses in *vps-50* mutants as compared to wild-type animals (Figure 5I). We postulate that mutation of *vps-50* has a broad impact on neuropeptides and that the behavioral defects of *vps-50* mutants are the result of the perturbation of one or of multiple neuropeptides.

We further compared *vps-50* and *rab-2* mutants using a transgene that expresses the dense-core vesicle marker IDA-1::GFP [13]. As previously reported, *rab-2* mutants have increased levels of IDA-1::GFP in cell bodies and lower levels of IDA-1::GFP at synapses, reflecting their defect in dense-core vesicle maturation. By contrast, *vps-50* mutants had elevated levels of IDA-1::GFP in both cell bodies and at synapses (Figures 5F and 5G), indicating that *vps-50* and *rab-2* both affect dense-core vesicle maturation and do so with some differences.

Neuropeptides are produced from proproteins, which in *C. elegans* are cleaved into peptides by the proprotein convertase 2 enzyme EGL-3 [18]. We asked whether *vps-50* mutants are defective in neuropeptide processing. We examined FLP-3::Venus from protein extracts using immunoblotting and observed that *vps-50* mutants had reduced levels of FLP-3 and that the ratio of processed to unprocessed FLP-3 was significantly lower than in the wild-type (Figure 5H).

In short, our results suggest that the behavioral defects of *vps-50*, *unc-31*, and *rab-2* mutants are similar because all three are low in neuropeptide release. However, *vps-50* mutants are distinct, because unlike *unc-31* mutants they did not accumulate neuropeptides at synapses and unlike *rab-2* mutants they had elevated levels of the dense-core vesicle protein IDA-1::GFP at synapses.

VPS-50 and Its Murine Homolog Affect Synaptic and Dense-Core Vesicle Acidification

To identify physical partners of VPS-50, we purified recombinant VPS-50 sections fused to glutathione-S-transferase (GST-VPS-50) and probed a protein extract from wild-type *C. elegans* in a pull-down experiment. Using mass spectrometry, we identified VHA-15, a homolog of the H subunit of the V-ATPase complex [21], as a possible VPS-50 interactor (data not shown). We confirmed the interaction between VPS-50 and VHA-15, which might be direct or indirect, using the yeast two-hybrid system (Figure 6A). The V-ATPase complex is a proton pump that acidifies cellular compartments, including synaptic and dense-core vesicles, the lysosome, and the *trans*-Golgi apparatus [21, 23]. In neurons, V-ATPase activity is required for loading neurotransmitters into synaptic vesicles [24], and its disruption can impair neuropeptide processing because of a failure in acidifying vesicles to the pH optimum of processing enzymes [25]. Given the interaction between VPS-50 and VHA-15, we postulated that VPS-50 regulates or responds to the activity of the V-ATPase complex responsible for the acidification of synaptic and dense-core vesicles.

To investigate the effect of impaired V-ATPase function in neurons, we examined mutants defective in the V-ATPase subunit UNC-32, which is required for synaptic vesicle acidification [22, 26], using the FLP-3::Venus and IDA-1::GFP reporters described above. *unc-32* mutants had low neuropeptide levels and high IDA-1::GFP levels at synapses, molecular defects similar to those of *vps-50* mutants (Figures S5A–S5D). (*unc-32* mutants are small, sickly, and severely impaired in locomotion [Figure S5E]. For this reason, *unc-32* mutants cannot be assessed for locomotory responses to external cues for comparison with *vps-50* mutants.) We then analyzed the acidification of synaptic and dense-core vesicles in intact worms by expressing

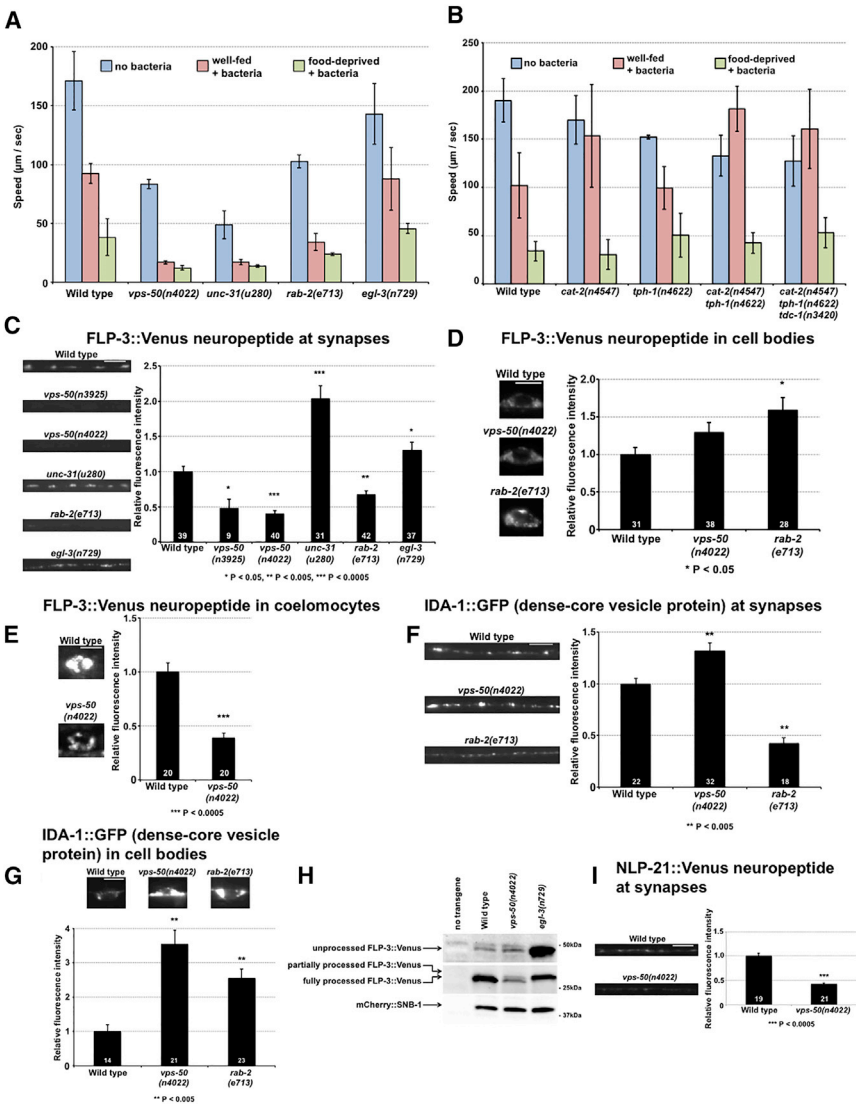

Figure 5. *vps-50* Disruption Reduces Neuropeptide Levels and Impairs Neuropeptide Processing

(A) Modulation of locomotion in response to the presence of food and past feeding experience. Like *vps-50* mutants, *unc-31* (CADPS2) and *rab-2* (Rab2) mutants, which are defective in dense-core vesicle release and maturation, respectively, behave as though they had been food deprived even when well fed; *egl-3* (PC2) mutants are more similar to wild-type animals. n = 4 plates for the wild-type; n = 3 plates for all other genotypes.

(B) Mutant animals defective in the synthesis of biogenic amines (*cat-2*: dopamine; *tph-1*: serotonin; *tdc-1*: tyramine and octopamine) behave differently when well fed or food deprived, unlike *vps-50* mutants. n = 10 plates for the wild-type; n = 3 plates for all other genotypes.

(C) *vps-50* mutants, like *rab-2* mutants, show reduced FLP-3::Venus neuropeptide levels in the *C. elegans* dorsal nerve cord. *unc-31* and *egl-3* mutants show elevated neuropeptide levels at synapses.

(D) *vps-50* mutants do not significantly accumulate FLP-3::Venus neuropeptides in neuronal cell bodies.

(E) *vps-50* mutants have reduced levels of FLP-3::Venus neuropeptides in coelomocytes.

(F) *vps-50* mutants do not have a dense-core vesicle maturation defect identical to that of *rab-2* mutants based on the dense-core vesicle marker IDA-1::GFP in the *C. elegans* dorsal nerve cord.

(G) *vps-50* mutants, like *rab-2* mutants, abnormally accumulate IDA-1::GFP in ventral nerve cord cell bodies.

(H) *vps-50* mutants have reduced levels of the neuropeptide FLP-3 as well as reduced FLP-3 processing. Immunoblots of *C. elegans* protein extracts showing the levels of processed and unprocessed neuropeptide FLP-3::Venus and the constant levels of the synaptobrevin reporter mCherry::SNB-1. The transgene *cels61* expressed both FLP-3::Venus and mCherry:SNB-1 from the *unc-129* promoter. Mutants for the proprotein convertase 2 homolog EGL-3 had no detectable fully processed FLP-3 neuropeptides.

(I) *vps-50* mutants show reduced NLP-21::Venus neuropeptide levels in the *C. elegans* dorsal nerve cord.

Scale bars, 5 µm. Bar graphs (A and B), means ± SDs. Bar graphs (C–G and I), n values (number of animals) are indicated on the bars; representative fluorescence micrographs and quantification are shown; means ± SEMs. See also Figure S4.

synapto-pHluorin (SpH) using the *unc-17* promoter. SpH is a fusion of the synaptic-vesicle protein synaptobrevin with the pH-sensitive GFP reporter pHluorin, and the pHluorin moiety is localized to the vesicular lumen, where it can be used to assay vesicle pH [27, 28]. SpH has been used to study the effects of mutations in the V-ATPase complex on *C. elegans* GABAergic neurons [22]. *vps-50* mutants, like *unc-32* mutants, showed increased SpH fluorescence, indicating that *vps-50* mutants are defective in vesicle acidification (Figures 6B and 6C). *unc-32* mutants share several aspects of the *vps-50* mutant phenotype. However, whereas *unc-32* mutants have low levels of synaptobrevin (SNB-1) at synapses, *vps-50* mutants have normal levels (Figure 6C). Because SpH is an SNB-1::pHluorin fusion, *unc-32* likely has a greater effect than *vps-50* on V-ATPase complex activity. The increased SpH fluorescence in *vps-50* mutant animals is unlikely to be the result of SpH missorting in these mutants, because SpH colocalizes with the vesicular acetylcholine transporter UNC-17 in both wild-type and *vps-50* mutant animals (Figure S5F) and SpH localization to dorsal cord synapses in *vps-50* mutants is dependent on UNC-104/KIF1A, as in the wild-type (Figure S5G). Impaired endocytosis at synapses could also lead to increased SpH fluorescence by causing an accumulation of SpH at the plasma membrane. To ask whether *vps-50* mutants fail to recycle SpH, we compared them to mutants for *unc-11*, the AP180 homolog; *unc-11* mutants fail to recycle synaptic vesicle-associated proteins such as SpH and show a diffusion of SpH (and SNB-1) all along the plasma membrane [29]. The diffusion of synaptic vesicle-associated proteins in *unc-11* mutants is independent of UNC-104/KIF1A function, as *unc-11; unc-104* double mutants similarly

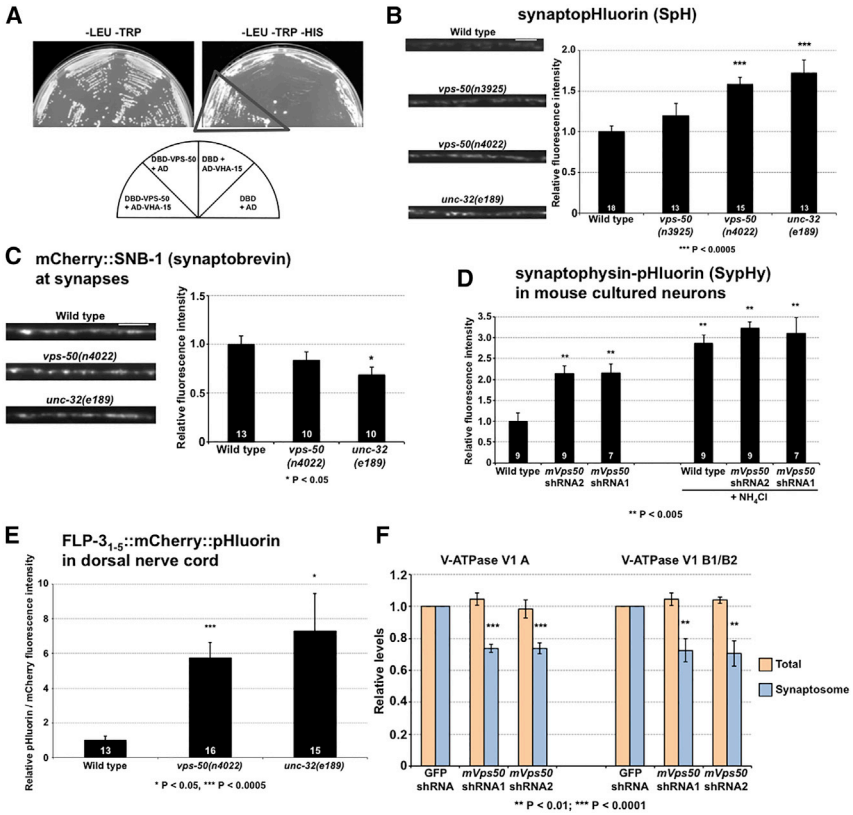

Figure 6. Disruption of *vps-50* in *C. elegans* or of Its Murine Homolog *mVps50* in Mouse Cultured Neurons Similarly Impairs Synaptic Vesicle Acidification

(A) VPS-50 can associate with the V-ATPase subunit VHA-15 in the yeast two-hybrid assay. Growth occurred on media lacking histidine (dark triangle). AD, activation domain; DBD, DNA-binding domain.

(B) *vps-50* mutants have a synaptic vesicle acidification defect. Representative micrographs and quantification of synapto-pHluorin (SpH) fluorescence levels. SpH fluorescence is quenched by acidic pH; thus, increased fluorescence levels correspond to increased pH. Mutants defective in the V-ATPase complex subunit gene *unc-32* were used as an acidification-defective control [22].

(C) *vps-50* mutants did not have elevated levels of synaptobrevin (SNB-1) at synapses, indicating that the higher SpH (an SNB-1::pHluorin fusion) fluorescence levels observed in *vps-50* and *unc-32* mutants were not caused by elevated levels of SpH at synapses. Representative fluorescence micrographs and quantification of mCherry::SNB-1 levels at synapses.

(D) Knockdown of *mVps50* in mouse primary cultured cortical neurons led to a synaptic vesicle acidification defect. Quantification of SypHy (synaptophysin-pHluorin fusion) fluorescence levels with or without knockdown of *mVps50*. Higher fluorescence levels correspond to higher pH. SypHy expression levels in wild-type and *mVps50* knocked-down neurons are similar, as addition of NH_4Cl to increase the intravesicular pH to 7.4 led to similar SypHy fluorescence levels in both.

(E) *vps-50* mutants have a dense-core vesicle acidification defect. pHluorin and mCherry fluorescence intensities were quantified from the FLP-3_{1-5}::mCherry::pHluorin reporter. An increased pHluorin/mCherry fluorescence ratio indicates increased pH. Mutants defective in the V-ATPase complex subunit gene *unc-32* were used as an acidification-defective control.

(F) Knockdown of *mVps50* in mouse primary cultured cortical neurons reduces the amount of V-ATPase (V1) subunits A and B in the synaptosomal fraction. Levels of V-ATPase soluble subunits A and B were quantified in total protein extracts and in synaptosomal fractions in wild-type and *mVps50* knocked-down primary cultured neurons. n = 6.

Scale bars, 5 μm. Bar graphs, n values (number of animals or neurons) are indicated on the bars; means ± SEMs. See also Figure S5.

show diffusion of SNB-1 along the plasma membrane in neuronal processes [29]. By contrast, we observed no such diffusion of SpH in *unc-104; vps-50* double mutants (Figure S5G). We conclude that *vps-50* controls the acidification of vesicles rather than affect the levels of surface SpH.

To test whether the role of VPS-50 in vesicle acidification is evolutionarily conserved, we used small hairpin RNAs (shRNAs) to knock down *mVps50* levels in mouse primary cultured cortical neurons transfected with a synaptophysin-pHluorin fusion (SypHy) [30]. We observed that neurons reduced in mVPS50 levels had higher SypHy fluorescence levels than wild-type neurons (Figure 6D). Most SypHy signal, like the SpH signal observed in *C. elegans*, is from synaptic vesicles, which are more abundant than dense-core vesicles. Thus, disruption of *mVps50* led to an acidification defect of synaptic vesicles in murine neurons. This observation further establishes the evolutionarily conserved functions of VPS-50 and mVPS50. Increasing the intravesicular pH to 7.4 using NH_4Cl (see the Experimental Procedures) increased the SypHy fluorescence of wild-type and *mVps50* knocked-down neurons to similar levels. Thus, the high SypHy fluorescence observed in neurons depleted for *mVps50* resulted from a defect in vesicle acidification and not from a difference in SypHy expression, because neutralizing the pH of the vesicular lumen resulted in comparable SypHy fluorescence levels for wild-type and *mVps50* knocked-down neurons.

Because the signals from the SpH and SypHy reporters are predominantly from synaptic vesicles, we developed a new reporter to assess the acidification of dense-core vesicles specifically. We fused both mCherry and pHluorin to the C-terminal end of a neuropeptide reporter encoding the first five neuropeptides of the *flp-3* gene (FLP-3_{1-5}::mCherry::pHluorin); neuropeptides are found in dense-core vesicles, but not in synaptic vesicles. mCherry, which is largely pH insensitive, provides an internal control. We expressed this reporter in cholinergic neurons and used the ratio of the pHluorin/mCherry fluorescence intensities as a measure of pH. (A previous study showed that such a pHluorin/mCherry ratio indicates pH [31].) The intramolecular ratiometric nature of our reporter is important, because we use this neuropeptide reporter in mutants that have altered neuropeptide levels; this reporter allows us to normalize for these different neuropeptide levels. That the FLP-3_{1-5}::mCherry::pHluorin reporter is indeed vesicle associated is confirmed by the observation that its transport to the dorsal nerve cord is

UNC-104/KIF1A dependent (data not shown); UNC-104/KIF1A transports dense-core and synaptic vesicles. Furthermore, the FLP-3_{1-5}::mCherry::pHluorin reporter can be observed in coelomocytes, indicating its release (see above) and establishing that it accurately reflects neuropeptide trafficking. Because FLP-3 is a soluble peptide, the FLP-3_{1-5}::mCherry::pHluorin reporter should be localized to the lumen of dense-core vesicles, unlike the SpH reporter (a fusion between pHluorin and the membrane protein synaptobrevin), which is localized to both synaptic vesicles and the plasma membrane. Thus, the FLP-3_{1-5}::mCherry::pHluorin reporter yields a more specific signal for intravesicular acidity than does SpH. Mutants for *vps-50* and the V-ATPase subunit gene *unc-32* showed impaired dense-core vesicle acidification, as their pHluorin/mCherry fluorescence intensity ratios were higher than that of wild-type animals (Figure 6E).

mVPS50 Functions in the Assembly of the V-ATPase Complex

Taken together, our results demonstrate that *C. elegans vps-50* functions in the maturation and acidification of dense-core vesicles and through the acidification process affects neuropeptide signaling. Given that VPS-50 interacts with VHA-15, the H subunit responsible for the assembly of the soluble and membrane-bound moieties of the complex, we hypothesized that through its interaction with VHA-15, VPS-50 might function in the assembly of the V-ATPase complex onto synaptic and dense-core vesicles, thus regulating vesicle acidification. To test this hypothesis, we analyzed the presence of two of the soluble subunits of the V-ATPase complex, V1 subunits A and B, on synaptic vesicles in control mouse cultured primary neurons and in neurons knocked down for *mVps50*. The rationale for this experiment was that these soluble A and B subunits would be present on the membrane of synaptic vesicles only when the V-ATPase complex is fully assembled. We purified the synaptosomal fraction and analyzed the amounts of V-ATPase V1 A and B subunits by immunoblotting. We found that knockdown of *mVps50* decreased the levels of synaptosomal V-ATPase subunits A and B as compared to control fractions (Figure 6F). The total levels of these subunits were not affected in a whole-cell lysate, indicating that the decreased synaptosomal levels observed in the *mVps50* knockdown were not caused by generally lower V-ATPase V1 A and B subunit levels (Figure 6F). Taken together, our results suggest that *C. elegans* VPS-50 and its mammalian homologs are required for the proper assembly of the V-ATPase subunits into a functional holoenzyme, a process necessary for vesicle acidification. Alternatively, it is possible that VPS-50 acts in the sorting of the V-ATPase subunits to their site of assembly, which could lead to the formation of abnormal vesicles that are impaired in acidification.

DISCUSSION

We propose that VPS-50 regulates the behavioral state of *C. elegans* by controlling dense-core vesicle maturation and acidification and thereby modulating neuropeptide signaling. VPS-50 and its mammalian homologs likely share an evolutionarily conserved function in V-ATPase complex assembly or sorting, leading to the generation of immature or otherwise abnormal dense-core vesicles impaired in vesicular acidification.

The V-ATPase complex functions broadly to acidify cellular compartments, and the differential expression of subunit isoforms can confer cellular specificity to the localization and function of the complex [21]. It is possible that VPS-50 and its homologs regulate the V-ATPase complex specifically in neurons. VPS-50 might function in vesicle acidification as early as the *trans*-Golgi, from which dense-core vesicles are generated. Interestingly, recent studies have shown that fly and human VPS50 can associate with components of the Golgi-associated retrograde protein (GARP) complex, which functions in retrograde transport from endosomes to the *trans*-Golgi, suggesting that *vps-50* might act in protein sorting [32–35]. GARP consists of four proteins: VPS51, VPS52, VPS53, and VPS54. VPS50 replaces VPS54 in an alternative complex, the endosome-associated recycling protein (EARP) complex, which shares the VPS51, VPS52, and VPS53 subunits with GARP. Based on those interactions, the murine and human proteins have been named VPS50. (We note that VPS50 is referred to as Syndetin [34] or VPS54L [35] in two of these studies.) These reports further suggest that VPS50 localizes in part to recycling endosomes and that knockdown of *VPS50* leads to impaired recycling of proteins to the plasma membrane. These observations are consistent with our findings that *vps-50* mutants show altered neuropeptide and dense-core vesicle protein levels at synapses and that *mVps50*-depleted neurons show impaired assembly or sorting of V-ATPase complex subunits. We suggest that the EARP complex could function in the maturation of dense-core vesicles.

unc-31 functions in dense-core vesicle release [12]. Mutations in *vps-50* and *unc-31* both lead to low levels of neuropeptide secretion as well as to similar behavioral phenotypes. Disruption of CADPS2, the mammalian homolog of *unc-31*, in both mice and humans has been linked to autism spectrum disorders [36, 37]. In addition, a deletion spanning only *hVPS50* (the human homolog of *vps-50*) and a second gene, *CALCR* (calcitonin receptor), has been reported in an autistic patient [38]. We suggest that VPS-50 plays a fundamental role in synaptic function and in the modulation of behavior and that an understanding of *vps-50* and its mammalian homologs might shed light on mechanisms relevant to human behavior and possibly to neuropsychiatric disorders, including autism spectrum disorders.

EXPERIMENTAL PROCEDURES

Behavioral Analysis

For locomotion analyses, young adult worms were washed off a plate with S Basal medium and allowed to sediment in a 1.5-ml tube. Liquid was removed by aspiration, and worms in about 100 μl of S Basal were transferred to the center of an assay plate seeded with an *Escherichia coli* OP50 lawn covering the entire surface. For tracking in the absence of bacteria, worms were washed an extra time in S Basal before transfer to an unseeded plate. After 30 min in the absence of bacteria, worms were washed off with S Basal and transferred to a new seeded plate. We used a worm tracker [39] to record 10-min videos. The average speed of the population between minutes 3 and 4 of the recording is reported. The developmental stages of laid eggs were scored as described [40]. For pharyngeal pumping rates, animals were recorded at 25 frames/s using a Nikon SMZ18 microscope with a DS-Ri2 camera and the videos were scored for pumping events during a 10-s window.

Microscopy and Immunohistochemistry

For analysis of coelomocyte fluorescence, worms were immobilized in 30 mM NaN_3 on nematode growth medium (NGM) pads, and z stacks of images were

acquired using a Zeiss LSM 510 confocal microscope. Maximal-intensity projections of the coelomocytes were analyzed using ImageJ (NIH). Worms expressing other fluorescent reporters were immobilized with polystyrene beads on pads made of 10% agarose in M9 and imaged using a Zeiss Axioskop 2 microscope and a Hamamatsu ORCA-ER camera, with the exception of worms expressing the FLP-3::mCherry::pHluorin fusion, which were imaged using a Nikon Eclipse *Ti* microscope and a Princeton Instruments PIXIS 1024 camera. Images were analyzed using ImageJ. Fluorescence intensities were quantified using a selected region of interest (ROI) from which we subtracted a background of equal size from a nearby region. The dorsal nerve cord was imaged near where the posterior gonad arm turns. For quantification of the FLP-3::mCherry::pHluorin fusion fluorescence intensities, the "subtract background" option of ImageJ was used prior to selecting ROIs as above. For immunohistochemistry, worms were washed off plates in PBS 1× and transferred to a 1.5-ml tube. Animals were washed three times and frozen in liquid nitrogen in about 150 μl of PBS 1×. Aliquots were thawed and pressed between two glass slides and placed on dry ice for 10 min. The glass slides were pulled apart and covered in ice-cold methanol in 50-ml tubes. Worms were washed off the glass slides using a Pasteur pipette, and the glass slides were removed from the tube. Tubes were centrifuged for 5 min at 3,700 rpm. Worms were retrieved using a Pasteur pipette and transferred to a clean 1.5-ml tube. Methanol was removed. Worms were incubated in acetone for 5 min on ice. Worms were rehydrated three times in PBS 1× and incubated overnight at 4°C with rabbit monoclonal anti-GFP antibody (1:100) (Invitrogen) and mouse monoclonal anti-SNB-1 (1:100) antibody or mouse anti-UNC-17 (1:100) antibody (gift from J. Rand). Secondary antibodies were goat anti-rabbit and anti-mouse antibodies coupled with Alexa 594 and Alexa 488 (1:2,500), respectively (Invitrogen). Images were acquired using a Zeiss Axioskop 2.

Primary Hippocampal and Cortical Neuron Cultures

All manipulations were performed in accord with the guidelines of the MIT Institutional Animal Care and Use Committee. Primary neuron cultures were prepared from embryonic day 15 (E15) mice. Hippocampus or cortex was dissected and treated with papain (Worthington) and DNaseI (Sigma) for 10 min at 37°C and triturated with a fire-polished Pasteur pipette. Cells were plated at a density of 5×10^4 cells/cm^2 on coverslips or plastic plates that were pre-coated with alpha-laminin and poly-D-lysine and cultured in Neurobasal medium supplemented with B-27.

Immunocytochemistry and Immunohistochemistry of Mouse Neurons

For immunocytochemistry, mouse cultured neurons were fixed with 4% paraformaldehyde in PBS for 10 min, permeabilized, and blocked with 5% goat serum and 0.3% Triton X-100 in PBS for 1 hr. After incubation with primary antibodies overnight at 4°C and with secondary antibodies for 1 hr at room temperature, coverslips were mounted with Fluoromount-G (Electron Microscopy Sciences). z stack images were taken using a Nikon PCM 2000 or C2 confocal microscope with a 60× oil objective (numerical aperture [N.A.] 1.4) at 0.5-μm z intervals.

For immunohistochemistry, vesicular GABA transporter (VGAT)-Venus mice were perfused with 4% paraformaldehyde in PBS, cryoprotected in 30% sucrose, and sectioned at 60 μm on a freezing microtome. Sagittal sections were permeabilized and blocked in 5% goat serum and 1% Triton X-100 in PBS. Sections were incubated with primary antibodies overnight at 4°C and secondary antibodies for 2 hr at room temperature and mounted with Fluoromount-G. z stack images were taken using a Nikon PCM 2000 confocal microscope with a 10× objective (N.A. 0.5) at 10-μm z intervals. The figures presented are projections from these confocal z stacks. Image analysis was performed by ImageJ. Antibodies used were mVPS50/CCDC132 (rabbit; Sigma), Chromogranin C (mouse; Abcam), neuropeptide Y (sheep; Millipore), GFP (rat; Nacalai), NeuN (mouse; Millipore), GM130 (mouse; BD Biosciences), Golgin-97 (mouse; Santa Cruz), and TGN-43 (sheep; Serotec). Secondary antibodies were goat anti-mouse, anti-rabbit, anti-rat, or anti-sheep conjugated with Alexa 488, Alexa 543, or Alexa 633 (Invitrogen).

Transfection and Confocal Imaging of SypHy

Cultured cortical neurons were cotransfected with SypHy and shRNA or control plasmids using Lipofectamine 2000 (Invitrogen) at DIV (days in vitro) 5–7 and imaged using a Nikon PCM 2000 or C2 confocal microscope with a 60× water objective (N.A. 1.0) at DIV 10–14. Imaging was performed using a modified Tyrode's solution containing 150 mM NaCl, 4 mM KCl, 2 mM $MgCl_2$, 2 mM $CaCl_2$, 10 mM glucose, and 10 mM HEPES (pH 7.4); 50 μM amino-5-phosphonovalerate (AP-5) and 10 μM 6-cyano-7-nitroquinoxaline-2,3-dione (CNQX) were added to prevent excitotoxicity. A modified Tyrode's solution substituting 50 mM NaCl with 50 mM NH_4Cl was used to confirm the expression level of SypHy, as described previously [41].

Statistical Tests

For colocalization experiments, Pearson's correlation coefficients were obtained using the Coloc2 plugin in ImageJ. An ROI was drawn to include the cell bodies and dendrites. Bar graph comparisons were performed using Student's t test, and multiple comparisons were corrected using the Holm-Bonferroni method.

Additional experimental procedures are available in the Supplemental Information.

SUPPLEMENTAL INFORMATION

Supplemental Information includes Supplemental Experimental Procedures and five figures and can be found with this article online at http://dx.doi.org/10.1016/j.cub.2016.01.049.

AUTHOR CONTRIBUTIONS

N.P., Y.M., A.F., D.T.O., M.A., C.L.P., M.C.-P., and H.R.H. designed the experiments and analyzed the data. N.P., Y.M., M.A., C.L.P., M.C.-P., and H.R.H. wrote the manuscript. N.P., Y.M., A.F., D.T.O., M.A., and C.L.P. performed the experiments.

ACKNOWLEDGMENTS

We thank R. Droste for determining DNA sequences; N. An for strain management; G. Miesenböck, L. Lagnado, Y. Yanagawa, A. Miyawaki, P. Chartrand, K. Miller, J. Rand, J.T. August, M. Nonet, and the Developmental Studies Hybridoma Bank for reagents; and D. Denning, D. Ma, N. Bhatla, and S. Luo for discussions. N.P. was supported by a postdoctoral fellowship from the Natural Sciences and Engineering Research Council of Canada (NSERC). A.F. was supported by an NIH NRSA postdoctoral fellowship. This work was supported by NIH grant GM024663 (to H.R.H.) and by a grant from the Simons Foundation to the Simons Center for the Social Brain at MIT (to H.R.H. and M.C.-P.). H.R.H. is the David H. Koch Professor of Biology at MIT and an Investigator of the Howard Hughes Medical Institute.

Received: February 24, 2015
Revised: November 20, 2015
Accepted: January 21, 2016
Published: March 3, 2016

REFERENCES

1. Sawin, E.R., Ranganathan, R., and Horvitz, H.R. (2000). *C. elegans* locomotory rate is modulated by the environment through a dopaminergic pathway and by experience through a serotonergic pathway. Neuron *26*, 619–631.
2. Ranganathan, R., Sawin, E.R., Trent, C., and Horvitz, H.R. (2001). Mutations in the *Caenorhabditis elegans* serotonin reuptake transporter MOD-5 reveal serotonin-dependent and -independent activities of fluoxetine. J. Neurosci. *21*, 5871–5884.
3. Ailion, M., Hannemann, M., Dalton, S., Pappas, A., Watanabe, S., Hegermann, J., Liu, Q., Han, H.-F., Gu, M., Goulding, M.Q., et al. (2014). Two Rab2 interactors regulate dense-core vesicle maturation. Neuron *82*, 167–180.
4. Swaab, D.F. (2004). Neuropeptides in hypothalamic neuronal disorders. Int. Rev. Cytol. *240*, 305–375.

5. Sakurai, T. (2007). The neural circuit of orexin (hypocretin): maintaining sleep and wakefulness. Nat. Rev. Neurosci. *8*, 171–181.
6. Hall, D.H., and Hedgecock, E.M. (1991). Kinesin-related gene *unc-104* is required for axonal transport of synaptic vesicles in *C. elegans*. Cell *65*, 837–847.
7. Nonet, M.L. (1999). Visualization of synaptic specializations in live *C. elegans* with synaptic vesicle protein-GFP fusions. J. Neurosci. Methods *89*, 33–40.
8. Matsumoto, Y., Imai, Y., Sugita, Y., Tanaka, T., Tsujimoto, G., Saito, H., and Oshida, T. (2010). CCDC132 is highly expressed in atopic dermatitis T cells. Mol. Med. Rep. *3*, 83–87.
9. Wang, Y., Kakizaki, T., Sakagami, H., Saito, K., Ebihara, S., Kato, M., Hirabayashi, M., Saito, Y., Furuya, N., and Yanagawa, Y. (2009). Fluorescent labeling of both GABAergic and glycinergic neurons in vesicular GABA transporter (VGAT)-Venus transgenic mouse. Neuroscience *164*, 1031–1043.
10. Park, J.J., Gondré-Lewis, M.C., Eiden, L.E., and Loh, Y.P. (2011). A distinct *trans*-Golgi network subcompartment for sorting of synaptic and granule proteins in neurons and neuroendocrine cells. J. Cell Sci. *124*, 735–744.
11. Avery, L., Bargmann, C.I., and Horvitz, H.R. (1993). The *Caenorhabditis elegans unc-31* gene affects multiple nervous system-controlled functions. Genetics *134*, 455–464.
12. Speese, S., Petrie, M., Schuske, K., Ailion, M., Ann, K., Iwasaki, K., Jorgensen, E.M., and Martin, T.F.J. (2007). UNC-31 (CAPS) is required for dense-core vesicle but not synaptic vesicle exocytosis in *Caenorhabditis elegans*. J. Neurosci. *27*, 6150–6162.
13. Edwards, S.L., Charlie, N.K., Richmond, J.E., Hegermann, J., Eimer, S., and Miller, K.G. (2009). Impaired dense core vesicle maturation in *Caenorhabditis elegans* mutants lacking *Rab2*. J. Cell Biol. *186*, 881–895.
14. Sumakovic, M., Hegermann, J., Luo, L., Husson, S.J., Schwarze, K., Olendrowitz, C., Schoofs, L., Richmond, J., and Eimer, S. (2009). UNC-108/RAB-2 and its effector RIC-19 are involved in dense core vesicle maturation in *Caenorhabditis elegans*. J. Cell Biol. *186*, 897–914.
15. Sulston, J., Dew, M., and Brenner, S. (1975). Dopaminergic neurons in the nematode *Caenorhabditis elegans*. J. Comp. Neurol. *163*, 215–226.
16. Sze, J.Y., Victor, M., Loer, C., Shi, Y., and Ruvkun, G. (2000). Food and metabolic signalling defects in a *Caenorhabditis elegans* serotonin-synthesis mutant. Nature *403*, 560–564.
17. Alkema, M.J., Hunter-Ensor, M., Ringstad, N., and Horvitz, H.R. (2005). Tyramine functions independently of octopamine in the *Caenorhabditis elegans* nervous system. Neuron *46*, 247–260.
18. Kass, J., Jacob, T.C., Kim, P., and Kaplan, J.M. (2001). The EGL-3 proprotein convertase regulates mechanosensory responses of *Caenorhabditis elegans*. J. Neurosci. *21*, 9265–9272.
19. Fares, H., and Grant, B. (2002). Deciphering endocytosis in *Caenorhabditis elegans*. Traffic *3*, 11–19.
20. Sieburth, D., Madison, J.M., and Kaplan, J.M. (2007). PKC-1 regulates secretion of neuropeptides. Nat. Neurosci. *10*, 49–57.
21. Toei, M., Saum, R., and Forgac, M. (2010). Regulation and isoform function of the V-ATPases. Biochemistry *49*, 4715–4723.
22. Ernstrom, G.G., Weimer, R., Pawar, D.R.L., Watanabe, S., Hobson, R.J., Greenstein, D., and Jorgensen, E.M. (2012). V-ATPase V1 sector is required for corpse clearance and neurotransmission in *Caenorhabditis elegans*. Genetics *191*, 461–475.
23. Moriyama, Y., Maeda, M., and Futai, M. (1992). The role of V-ATPase in neuronal and endocrine systems. J. Exp. Biol. *172*, 171–178.
24. Morel, N. (2003). Neurotransmitter release: the dark side of the vacuolar-H^+ATPase. Biol. Cell *95*, 453–457.
25. Jansen, E.J.R., Hafmans, T.G.M., and Martens, G.J.M. (2010). V-ATPase-mediated granular acidification is regulated by the V-ATPase accessory subunit Ac45 in POMC-producing cells. Mol. Biol. Cell *21*, 3330–3339.
26. Pujol, N., Bonnerot, C., Ewbank, J.J., Kohara, Y., and Thierry-Mieg, D. (2001). The *Caenorhabditis elegans unc-32* gene encodes alternative forms of a vacuolar ATPase *a* subunit. J. Biol. Chem. *276*, 11913–11921.
27. Miesenböck, G., De Angelis, D.A., and Rothman, J.E. (1998). Visualizing secretion and synaptic transmission with pH-sensitive green fluorescent proteins. Nature *394*, 192–195.
28. Miesenböck, G. (2012). Synapto-pHluorins: genetically encoded reporters of synaptic transmission. Cold Spring Harb. Protoc. *2012*, pdb.ip067827.
29. Nonet, M.L., Holgado, A.M., Brewer, F., Serpe, C.J., Norbeck, B.A., Holleran, J., Wei, L., Hartwieg, E., Jorgensen, E.M., and Alfonso, A. (1999). UNC-11, a *Caenorhabditis elegans* AP180 homologue, regulates the size and protein composition of synaptic vesicles. Mol. Biol. Cell *10*, 2343–2360.
30. Granseth, B., Odermatt, B., Royle, S.J., and Lagnado, L. (2006). Clathrin-mediated endocytosis is the dominant mechanism of vesicle retrieval at hippocampal synapses. Neuron *51*, 773–786.
31. Koivusalo, M., Welch, C., Hayashi, H., Scott, C.C., Kim, M., Alexander, T., Touret, N., Hahn, K.M., and Grinstein, S. (2010). Amiloride inhibits macropinocytosis by lowering submembranous pH and preventing Rac1 and Cdc42 signaling. J. Cell Biol. *188*, 547–563.
32. Huttlin, E.L., Ting, L., Bruckner, R.J., Gebreab, F., Gygi, M.P., Szpyt, J., Tam, S., Zarraga, G., Colby, G., Baltier, K., et al. (2015). The BioPlex network: a systematic exploration of the human interactome. Cell *162*, 425–440.
33. Wan, C., Borgeson, B., Phanse, S., Tu, F., Drew, K., Clark, G., Xiong, X., Kagan, O., Kwan, J., Bezginov, A., et al. (2015). Panorama of ancient metazoan macromolecular complexes. Nature *525*, 339–344.
34. Schindler, C., Chen, Y., Pu, J., Guo, X., and Bonifacino, J.S. (2015). EARP is a multisubunit tethering complex involved in endocytic recycling. Nat. Cell Biol. *17*, 639–650.
35. Gillingham, A.K., Sinka, R., Torres, I.L., Lilley, K.S., and Munro, S. (2014). Toward a comprehensive map of the effectors of Rab GTPases. Dev. Cell *31*, 358–373.
36. Sadakata, T., Washida, M., Iwayama, Y., Shoji, S., Sato, Y., Ohkura, T., Katoh-Semba, R., Nakajima, M., Sekine, Y., Tanaka, M., et al. (2007). Autistic-like phenotypes in Cadps2-knockout mice and aberrant CADPS2 splicing in autistic patients. J. Clin. Invest. *117*, 931–943.
37. Sadakata, T., and Furuichi, T. (2010). Ca(2+)-dependent activator protein for secretion 2 and autistic-like phenotypes. Neurosci. Res. *67*, 197–202.
38. Gai, X., Xie, H.M., Perin, J.C., Takahashi, N., Murphy, K., Wenocur, A.S., D'arcy, M., O'Hara, R.J., Goldmuntz, E., Grice, D.E., et al. (2012). Rare structural variation of synapse and neurotransmission genes in autism. Mol. Psychiatry *17*, 402–411.
39. Ma, D.K., Vozdek, R., Bhatla, N., and Horvitz, H.R. (2012). CYSL-1 interacts with the O_2-sensing hydroxylase EGL-9 to promote H_2S-modulated hypoxia-induced behavioral plasticity in *C. elegans*. Neuron *73*, 925–940.
40. Ringstad, N., and Horvitz, H.R. (2008). FMRFamide neuropeptides and acetylcholine synergistically inhibit egg-laying by *C. elegans*. Nat. Neurosci. *11*, 1168–1176.
41. Ashby, M.C., De La Rue, S.A., Ralph, G.S., Uney, J., Collingridge, G.L., and Henley, J.M. (2004). Removal of AMPA receptors (AMPARs) from synapses is preceded by transient endocytosis of extrasynaptic AMPARs. J. Neurosci. *24*, 5172–5176.